







Photochemical corneal cross-linking: Evaluating the potential of a hand-held biopen

Nadina Usseglio^{a,1} , Julia López de Andrés^{b,1} , Juan Antonio Marchal^{b,c} , Lorenzo Moroni^d, Daniel Nieto^{a,e,*} 

^a Advanced Biofabrication Laboratory - DNIETO LAB, Center for Interdisciplinary Chemical and Biology, CICA, University of La Coruña, Spain

^b Biopathology and Regenerative Medicine Institute (IBIMER), Centre for Biomedical Research (CIBM), University of Granada, Granada, E-18100, Spain

^c Instituto de Investigación Biosanitaria IBS GRANADA, University Hospitals of Granada- University of Granada, 18100, Granada, Spain

^d Complex Tissue Regeneration Department, MERLN Institute for Technology-Inspired Regenerative Medicine, Universiteitssingel 40, 6229ER, Maastricht, the Netherlands

^e Opportunius. Axencia Galega de Innovación, 15702, Santiago de Compostela, Spain

ARTICLE INFO

Keywords:

Hand-held biopen
Bioprinting
Photocrosslinking
Cornea repairing
Cornea Photocrosslinking

ABSTRACT

The generation of organized 3D tissue constructs that combines cells and photo-crosslinkable biomaterials has been demonstrated using a variety of 3D bioprinting technologies. These technologies have inspired the application for “*in situ*” bioprinting, resulting on hand-held tools called “Biopens” that can transfer bioprinting capabilities directly into the hands of the surgeons. Here, we have developed and validated a biopen for ophthalmological applications, specifically for corneal stromal regeneration using photochemical corneal crosslinking (CXL), as well as for cell bioprinting and, potentially, for corneal wound healing. We used the biopen to CXL, but also for fast crosslinking processes. Cytotoxicity, cell viability and immunofluorescence experiments were performed with human corneal stroma keratocytes (HCK) loaded inside the proposed bioink compositions. Photochemical cross-linking was performed to evaluate the biopen bioprinting functionality for corneal wound closure in porcine eyes. A full-thickness penetrating incision, 5 mm in length parallel to the limbus and perpendicular to the corneal surface, was made in the enucleated porcine cornea. The mechanical properties of cornea are imitated by tuning the proposed (GelMA/PEGDA/PI) bioink composition and crosslinking parameters, which envisage the potential for being translated to a clinical environment to corneal wound closure.

1. Introduction

The possibility of simultaneously controlling the deposition of biomaterials in combination with living cells and biological molecules is revolutionizing tissue engineering and regenerative medicine [1–3]. Bioprinting is currently considered as a highly promising technique in a variety of applications of regenerative medicine, including bone and cartilage regeneration [4–8], skin substitutes [9], cardiac valve [10] and cardiovascular system repair [11], craniofacial reconstruction [12], management of severe spinal conditions [13], musculoskeletal applications [14], hand surgery [15], reconstructive surgery [16], otorhinolaryngology [17] and dental applications [18].

The fundamental goal of having control over 3D bioprinting using

such bioinks is to mimic the natural biological microenvironments by creating 3D artificial tissues, where cells can function as well as they would in real tissues. The generation of organized 3D tissue constructs *via* a layer-by-layer deposition process (extrusion, inkjet and stereolithography) that combines cells and biomaterials has been demonstrated for a variety of applications [19]. The evolution of these technologies has inspired the application for “*in situ*” bioprinting resulting on other bioprinting tools called “Biopens” [21]. The ambition of such bioprinting hand-held tools is to develop a mobile version of a 3D bioprinter and put that capability of adding biomaterials and cells directly into the hands of the surgeon, just like the scalpel. Such hand-held biopens are emerging in the clinical environment as a biomedical tool for tissue sculpting. They have several advantages over

This article is part of a special issue entitled: Light-based 3D bioprinting applications published in Materials Today Bio.

* Corresponding author. Advanced Biofabrication Laboratory - DNIETO LAB, Center for Interdisciplinary Chemical and Biology, CICA, University of La Coruña, Spain.

E-mail address: daniel.nieto@udc.es (D. Nieto).

¹ Authors contributed equally to the manuscript.

<https://doi.org/10.1016/j.mtbio.2025.101512>

Received 7 July 2024; Received in revised form 24 November 2024; Accepted 20 January 2025

Available online 21 January 2025

2590-0064/© 2025 The Authors. Published by Elsevier Ltd. This is an open access article under the CC BY-NC-ND license (<http://creativecommons.org/licenses/by-nc-nd/4.0/>).

static procedures: 1) they are hand-held operated tools for precisely deposit biomaterials on living tissues “*in situ*”; 2) they are small devices that can be handled in/out of the surgical room; 3) their cost is relatively cheaper than other conventionally robotically manipulated systems; 4) they can be easily adapted to a variety of surgical sculpting; but they also have some limitations: their accuracy depends on the skill of the operator, which can lead to inconsistent results. In addition, the lack of detailed defect scanning and the absence of automation limit their ability to create complex or reproducible structures; and the ergonomics of the device can also influence user fatigue, affecting print quality during prolonged procedures [20].

Most of biopens are based on extrusion or spray with thermal, chemical, or light crosslinking [21]. UV-light based polymerization has been demonstrated to be a promising technique to accomplish crosslinks in connective living tissues, which can be easily incorporated into the biopens [22]. For ophthalmology applications, UV light photopolymerization has been used for CXL to treat the keratoconus (an ectatic disease of the cornea that mainly involves progressive curving and thinning) and for corneal injury repairing using UV light sensitive optical adhesives. CXL is a minimally invasive technique that is expected to stop the progression of corneal ectatic conditions by inducing crosslinking in the stromal collagen of the cornea [23]. The cornea layer is composed of collagen fibers and the binding force between the collagen fibers determines the strength and rigidity of the cornea. Crosslinking is activated using a non-toxic and soluble photo mediator, such as riboflavin (RF) and a UV wavelength, which must absorb enough to protect deeper layers of the eye. CXL using RF UV-A involves the use of RF eyedrops (a UV light absorbing yellow dye) that are soaked into the cornea. Once the cornea is fully impregnated with RF, UV light exposure in the presence of oxygen creates the conditions for new intermolecular bonds (crosslinks) to form.

Another ophthalmology promising application of the biopen is for corneal stroma defects repairing. Every year around 1.5 million new cases of corneal blindness are reported [24]. Only less than 5 % are treated by corneal transplantations (such a short percentage is because the donor tissue shortage and the high expense of transplantation surgery) [25]. Injuries and infections in the cornea are relatively common causes of stromal thinning and corneal scarring, which in the end can lead to loss of vision [26]. In severe or progressive cases of corneal stromal inflammation, losing the structure integrity can occur. Current standards of care for treatment of corneal stromal defects include the use of cyanoacrylate glue, tissue grafting, or corneal transplantation. Nevertheless, these methodologies generally have significant disadvantages. Adhesive biomaterials have arisen as a promising approach for the corneal stromal loss treatment, in particular for situations of emergency. Generally, such biomaterials must imitate the characteristics of the native cornea. An optimal adhesive biomaterial for repairing and regenerating the cornea must retain (1) a good biocompatibility and biodegradability, (2) mechanically stability with the suitable stiffness, (3) high transparency, (4) the ability to adhere strongly to the native tissue, (5) the ability to support cell and endogenous tissue regeneration, and (6) clinical compliance for ease of application and use (8).

We have developed a hand-held bioprinting tool to precisely add biomaterials into the eyes with the potential for being translated to a clinical in particular. The biopen was validated for corneal stromal regeneration using photochemical corneal crosslinking, for cell bioprinting and for cornea wound closure. Despite other biopens have been developed for surgical printing chondral wound sites, cartilage, and skin applications [27–29], to our knowledge there is no other hand-held automatized “biopen” using photochemical cross-linking for tissue cornea repairing or regeneration.

2. Materials and methods

2.1. Biopen

2.1.1. Design and fabrication

All the components of the biopen were designed using AUTODESK CAD Inventor software. The different parts were then prepared for printing with a 3D slicer software and printed using Raise 3D Pro plus printer. The material selected to print the biopen was Acrylonitrile Butadiene Styrene (ABS), which has good mechanical properties and good heat resistance up to 90 °C. ABS resins have been long valued for biomedical products because of their durability, toughness, exceptional purity and low residual monomers. The needle holder and the syringes/ biomaterial containers were connected using polyvinyl tubing. The tip holder with luer-lock connector supports multiple needle diameters. The Luer-lock connector also easily facilitates replacement of syringes. The syringes were connected to an air pump, which controls the pressure (1 kPa–200kPa) and so the material deposition rate. A UV photocuring light source and a 4k camera were integrated into the biopen to enable imaging of photocuring process.

2.1.2. Development

The biopen is based on a combination of extrusion with multiple tip diameters, a UV curing system and a 4K high-resolution camera (Fig. 1).

The overall bioprinting process using the biopen can be described as follows: a pneumatic system controls the biomaterial deposition rate by extruding the material inside a syringe/container. By increasing the air pressure more force is exerted on the piston placed at the back of the syringe, which pushes the biomaterial out through the tip. Extrusion is activated using a button in the biopen connected to an electronic valve, which opens/closes the airflow from an air pump. A regulator place at the air pump controls the pressure and so the material deposition rate. The tip/needle holder with Luer-lock connector supports multiple needle diameters. A variety of needle of different diameters (225, 250, 275 and 400 μm) have been used to demonstrate printability. In the front face of the biopen are placed a 4K wifi high resolution camera with illumination, for real-time imaging to visually assist during CXL procedure, and a UV light source (385 nm) with a lens to promote cross-linking of the extruded material, controlled by the electronic control circuit.

2.1.3. Printing process imaging

For real time visualization of the photochemical process, we used a high definition 4k 5 MP camera, with adjustable illumination LEDs and equipped with the function of real-time video viewing, video recording and picture capturing. The camera has a large focal range with zoom function and WIFI connection.

2.2. Biomaterials

To validate the biopen for cornea injury repairing we used a photocrosslinkable bioink (Fig. 2) of Polyethylene glycol diacrylate (PEGDA, Mn = 700, Sigma-Aldrich, St. Louis, MO, USA) and Gelatin methacryloyl (GelMA, Merck). As photoinitiator we used Lithium phenyl-2,4,6-trimethylbenzoylphosphinate (LAP), which has been demonstrated to be sensitive to blue light (absorption peak around 385 nm). For CXL, we used RF, also known as vitamin B2, which is a vital component of mitochondrial energy production. RF is a part of the co-enzyme flavin mononucleotide (FMN) and flavin adenine dinucleotide (FAD), involved in a number of oxidation and reduction reactions. In particular, we have used an ophthalmic solution for corneal crosslinking from RIBOCROSS, which contains RF (0.1 % w/v) instilled in the eye during irradiation of UV-A light as part of the surgical procedure of CXL. The composition is: RF 5” - Phosphate Sodium USP, equivalent to RF (0.1 % w/v), Dextran 500 (20 % w/v) and Aqueous Basse.

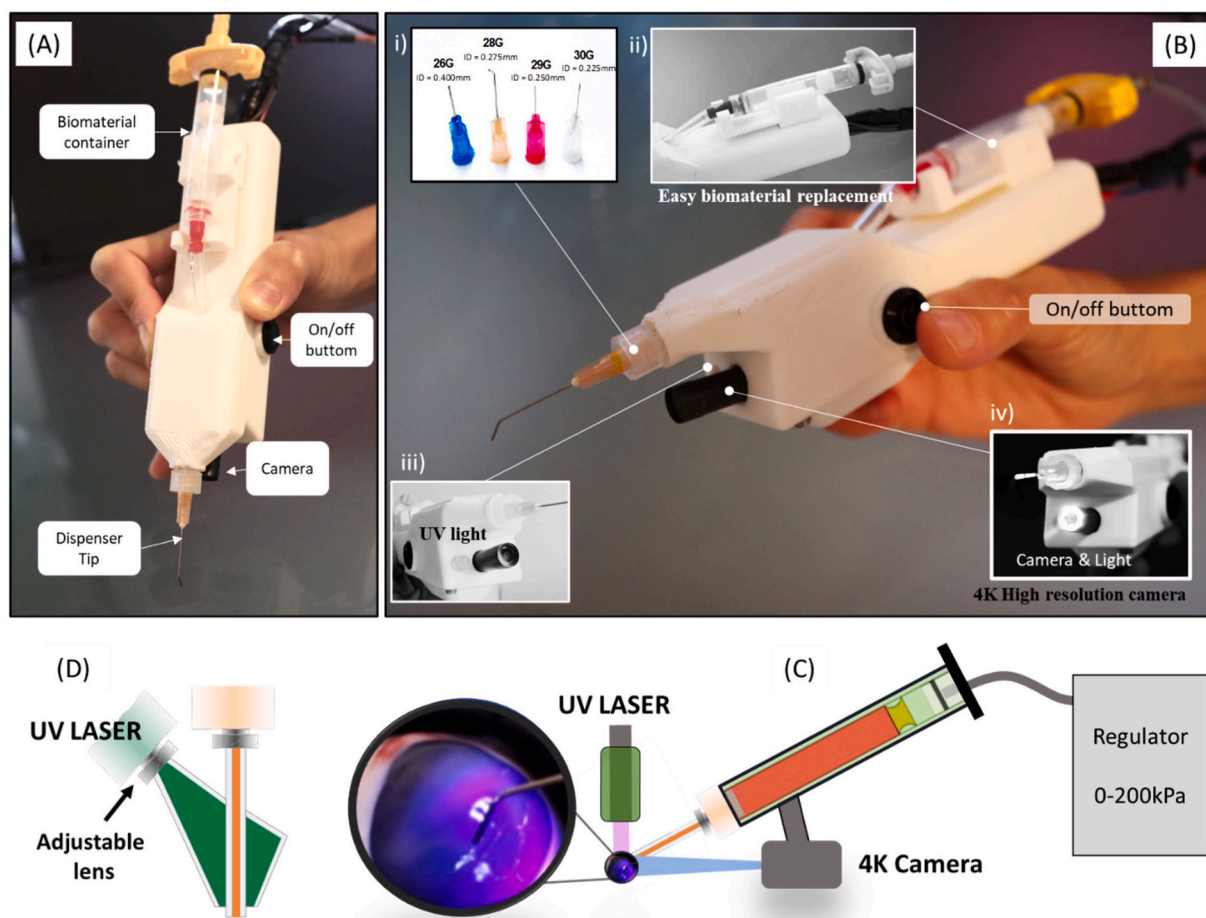


Fig. 1. Hand-held extrusion biopen. (A) Image of the biopen showing its ergonomic shape. (B) Image of the hand-held biopen with detailed images of components: i) available tips, ii) biomaterial syringe, iii) UV light source, iv) 4K high resolution camera. (C) Sketch showing the biopen elements and their interaction and (D) Sketch of tip/laser with adjustable lens.

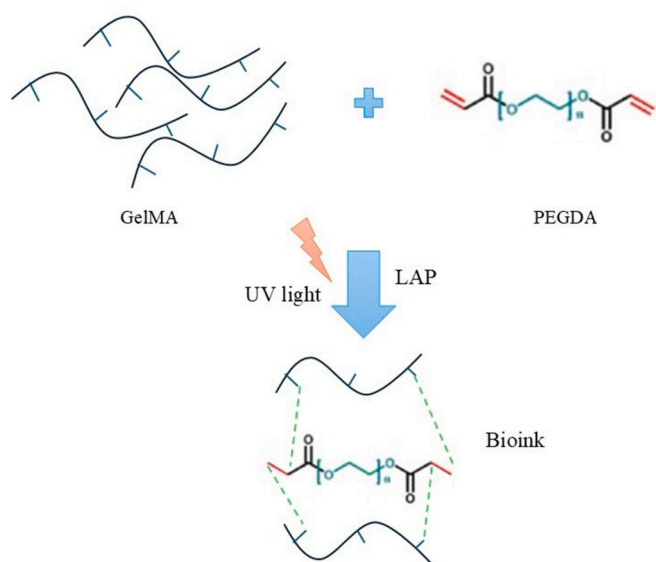


Fig. 2. Scheme of bioink structure.

2.3. Photocuring source

For photocuring the biomaterials (PEGDA/GelMA/PI) and for RF crosslinking we used a 385 nm light source integrated into the biopen

head. The source is orientated to concentrate the light in the working area with an intensity controller that can be modulated at different light power possibility the uses on traditional CXL (5.4 J/cm^2), as well in fast CXL approaches (7.2 J/cm^2). Light intensity was measured using a light power and Energy Meter Console (THOSLABS PM100D).

2.4. Cell printing

2.4.1. Cell sourcing

Human corneal stroma keratocytes (HCK) were purchased from Innoprot and used experimentally at passages 4–9. HCK lines were cultured with Fibroblast Medium (Innoprot) supplemented with 10 % Fetal Bovine Serum (FBS), Fibroblast Growth Supplement (Innoprot), and 1 % penicillin/streptomycin, in poly-lysine-coated culture flask under controlled conditions (37°C , 5 % CO_2). At 80 % of confluence, cells were subcultured using trypsin at 0.25 % (Sigma).

2.4.2. Preparation of bioinks

PEGDA/GelMa solution was prepared by dissolving GelMa (Sigma) powder in PBS, mixed with PEGDA, and then adding LAP (Apollo-Scientific) at a final concentration of 0.1 % (p/w). The bioink was mixed with the cells to a concentration of 1.5×10^6 cells/ml, and then loaded into the biopen and printed into sterile culture plates. Also, replicas of cell-loaded non-printed hydrogel were prepared as a control. As second control, HCK were seeded on imaging culture dishes (Ibidi) at initial concentration of 5.000–10.000 c/cm^2 . After printing, the hydrogels were covered with culture media and grown under controlled conditions (37°C , 5 % CO_2) for one week.

2.4.3. Cell proliferation assay

The proliferation rate of HCK encapsulated within the hydrogel and growing in monolayer was measured by colorimetric AlamarBlue® assay (Bio-Rad Laboratories, Inc., manufactured by Trek Diagnostic Systems, U.S.). Hydrogels and controls were incubated with 10µl/100 µl of AlamarBlue® solution for 1 h at 37 °C. At this time, fluorescence intensity was measured at an excitation wavelength of 530 nm and emission of 590 nm (Microplate Reader MB-580/530, Heales). Cell proliferation was analyzed on days 1, 3, 5 and 7 after printing. The absorbance data was represented as fold increase to day 0. Experiments were performed in triplicate (n = 3).

2.4.4. Cell viability assay

The viability of HCK in the biopen-printed hydrogel and controls was evaluated by the Live/dead assay (ThermoFisher™), at day 1, 3 and 7 after bioprinting. Briefly, samples were washed twice in PBS and stained

with calcine AM and EthD-I at the concentration indicated by the manufacturer, for 30' in dark. Images were taken by confocal microscopy (Nikon Eclipse Ti-E A1, USA) and analyzed using Image J Software. Live/dead cells were counted using cell counter macro of Image J Software (NIH) in 5 random sights of magnifying at 10× for 3 replicates of each sample (n = 3).

2.4.5. Immunofluorescence

The hydrogels were fixed in 4 % PFA (Sigma Aldrich) for 20 min at room temperature and then embedded in Tissue Freezing Medium (Leica Biosystems). Sections of 8 µm thickness were blocked with 3 % BSA in blocking buffer for 1 h at room temperature. Primary antibodies (*Anti-ALDH1A1*, anti-Keratocan, anti-αSMA, and anti-vimentin) were applied at a 1:200 dilution and incubated overnight at 4 °C. Following two PBS washes, the samples were incubated with a goat anti-rabbit IgG H&L Alexa Fluor® 488 secondary antibody (ab150077; Abcam) at a 1:500

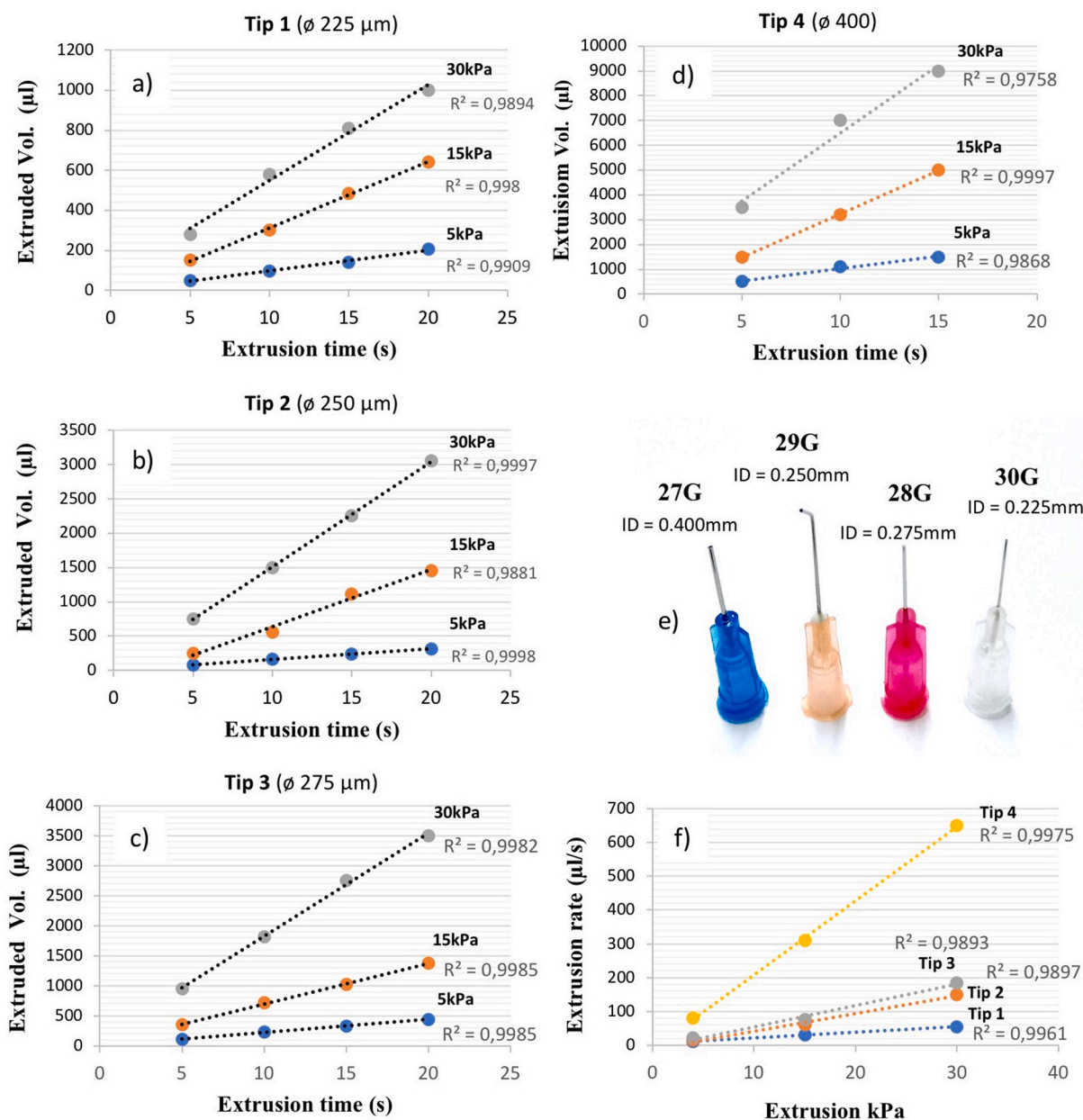


Fig. 3. Riboflavin deposition stability was determined by plotting the extruded volume of riboflavin versus extrusion time for a range on pressures (5 kPa, 15 kPa and 30 kPa) and for various tip/needle inner diameters: a) ø 225 µm, b) ø 250 µm, c) ø 275 µm and d) ø 400 µm. e) shows the different tips/needles used and f) the extrusion rates versus the applied pressures.

dilution for 2 h at room temperature. After two additional PBS washes, a mounting medium containing DAPI (Sigma Aldrich) was applied. Samples were imaged using a Leica DM 5500B microscope and processed with ImageJ software (v.2.13.1).

2.5. Statistical analysis

Results of cell viability and proliferation are represented as mean \pm SD from three replicas. ANOVA and Two-tailed Student's t-test was used to determine test significance between different conditions. A difference between the mean values for each group was considered statistically significant when the p value was less than 0.05.

2.6. Ethical considerations

The eyes used on this study are from death porcine and were obtained from a local provider. The authors declare that the data supporting the findings of this study are available within the paper.

3. Results

3.1. Cornea collagen crosslinking (CLX)

In order to determine the bioprinting capabilities of the biopen for precisely depositing RF drops onto the cornea, we determined the extrusion rate (volume of material/time) in function of the air pump pressure and the tip diameter. We have analyzed the RF deposition stability by measuring the extrusion parameters (pressure, time and volume) for a number of tip diameters including (225, 250, 275 and 400 μ m) that can be incorporated into the biopen head (Fig. 3).

Fig. 3 shows the extruded volume of RF versus the extrusion time for various applied pressures (5 kPa, 15 kPa and 30 kPa) for the biopen device with various tip diameters: 3a) 225 μ m, 3b) 250 μ m, 3c) 275 μ m, and 3d) 400 μ m. RF extrusion stability is reflected on the linear relationship between the extrusion time and the extrusion volume. In Fig. 3f) we plotted the extrusion rate versus the extrusion pressures. The extrusion rate increased linearly with the extrusion pressure for all the tip diameters. Tip 2 (250 μ m) and tip 3 (275 μ m) showed a closer slope; tip 1 (225 μ m) was slightly different while for tip 4 this difference was higher (it was expected as the diameter of tip 4 is considerable bigger than others). This can be related with the shear thinning rheological properties.

After selecting the appropriate extruding parameters (pressure: 5 kPa, extrusion rate: 10 μ l/s) to obtain a stable RF deposition process, we used the biopen for CXL with the Epi-on and Epi-off methodologies (Epi-on involves non-epithelium removed while Epi-off involves epithelium removing). The porcine eyes were collected from a local provider (butcher) within 3 h of slaughter. Eyes from each animal were delivered from the shop in separate plastic bags filled with water. The eyes were inspected carefully, any damaged globes or corneas were excluded from the study. Eyes were preserved in phosphate-buffered solution while awaiting for performing the studies. For de-epithelialized eyes, the surface epithelium was softly debrided with a scalpel blade, drops of

saline solution were used for moisturizing, resulting in a de-epithelialized area of about 8 mm diameter. Table 1 Summarize the experimental design and treatment groups. The study design include four separate treatment groups of porcine eyes. Group A included 4 pairs of eyes with epithelium removed and using Dresden Protocol. Group B included 4 with epithelium intact and using the Dresden Protocol. Group C included 4 eyes with epithelium intact removed and using fast cross-linking and Group D included 4 eyes with epithelium removed and using fast cross-linking.

Fig. 4 shows the CXL process and parameters using the hand-held biopen with the Epi-on and Epi-off methodologies. We compared the fast CXL process and the standard CXL protocol by analyzing the RF migration into the section corneal sample.

Fig. 4A confirms fluorophore migration within the sample for the cornea treated using the biopen with Epi-on CXL following the standard protocol (Dresden Protocol = UV dose of 5.4 J/cm² and exposure time = 30 min) and with Epi-on and Epi-off fast curing (UV dose of 7.2 J/cm² and exposure time = 4 min). It can be appreciated that the fast cross-linking resulted in a deeper fluorophore migration within the cornea when the epithelium was removed. Fig. 4B illustrates the eye globe during the CXL process. As it can be appreciated in subsection iii), fluorophore response to UV light was higher in the area where the epithelium was removed, due the stronger absorption of riboflavin in the Epi-off process.

3.2. Bioink printability and cell viability

To evaluate bioprinting capabilities of our biopen for biomaterial deposition into the cornea we used two biomaterials, PEGDA, which is the base material of the PEG-based adhesives used in cornea, and GelMA, which has been demonstrated to have low cell toxicity and is a reference bioink in bioprinting applications (the bionk was prepared using 0.05 % and 0.1 % LAP photoinitiator). We determined the extruded line for different pressures (5 kPa, 15 kPa and 30 kPa) using a tip of diameter 250 μ m (Fig. 5A and B).

The stiffness of different PEGDA/GelMA/PI mass concentration and degree of photocrosslinking was investigated. The results showed tunable stiffness values for the investigated bioink formulations: GelMA/PEGDA/PI (Fig. 5D). It was observed that when increasing the GelMA concentration from 0 % to 3 % w/v, the stiffness of PEGDA/GelMA samples also increase. By increasing the GelMA concentration from 3 % to 5 % w/v, had a combined decreasing and increasing consequence on the stiffness of PEGDA/GelMA/PI samples. The smallest average elastic modulus obtained was 22 \pm 1.0 kPa for 15 % v/v PEGDA 3 % w/v and GelMA for a concentration of 0.05 % w/v PI and the maximum modulus was 870 \pm 8 kPa for 35 % v/v PEGDA and 5 % w/v GelMA for a concentration with 0.1 % PI.

UV exposure time of 0.2 s was used for all the conditions. Increasing the PI concentration resulted on increasing the final construct stiffness. The elastic modulus values for each layer of the cornea have been reported to be: 7.5 \pm 4.2 kPa (anterior basement membrane), 109.8 \pm 13.2 kPa (Bowman's layer), 33.1 \pm 6.1 kPa (anterior stroma), and 50 \pm 17.8 kPa (Descemet's membrane) [39]. According to these numbers, the mechanical properties of human cornea could be imitated by tuning the proposed (GelMA/PEGDA/PI) bioink composition and crosslinking parameters.

As showed in Fig. 5A, B and 5E the thickness of the bioink depends on the applied pressure and the printing speed given by the operator's movement. The relation between the diameter of the lines and the extrusion pressure was found to be similar for both PEGDA and GelMA. Similar thicknesses were obtained for PEGDA and GelMA which ensure similar extrusion behaviour when PEGDA/GelMA/LAP bioinks are used.

In order to evaluate the feasibility of the biopen as an adequate system for cell administration and survival, the viability of encapsulated cells (HCK) was determined. Additionally, we evaluated the cell viability for a range of bioink GelMA/PEGDA combinations with 0.1 % LAP

Table 1

Summary of experimental design and treatment groups.

Group A	Group B	Group C	Group D
4 eyes	4 eyes	4 eyes	4 eyes
Epithelium removed	Epithelium intact	Epithelium intact	Epithelium removed
Dresden protocol	Dresden protocol	Fast cross-linking	Fast cross-linking
Riboflavine (RF)			
UV dose of 5.4 J/cm ²		UV dose of 7.2 J/cm ²	
Exposure time = 30 min		Exposure time = 4 min	
Hand-held biopen cross-linking			

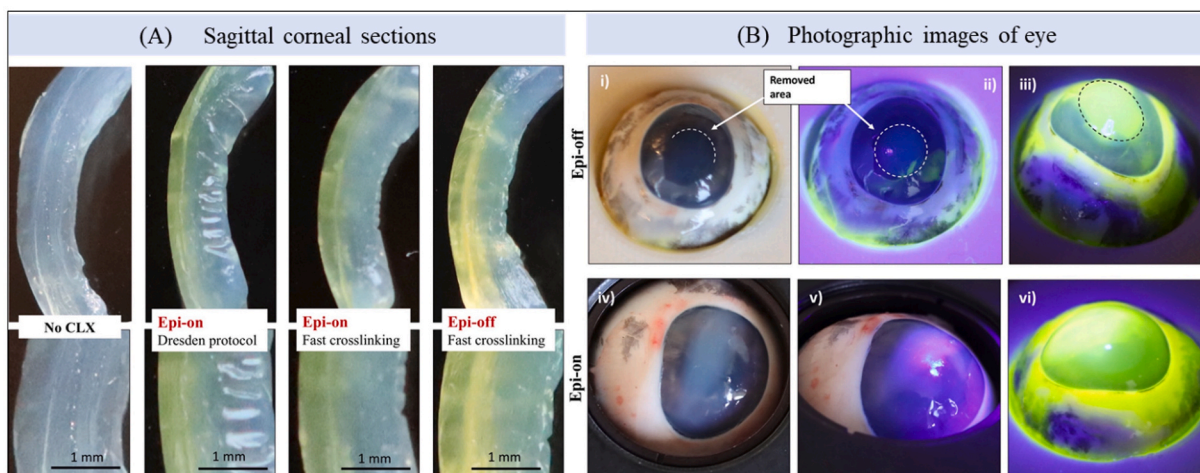


Fig. 4. (A) Color photographic of sagittal corneal sections illustrating the riboflavin absorption through the cornea for: i) non CXL, ii) Epi-on and Dresden protocol, iii) Epi-on and fast crosslink and iv) Epi-off and fast crosslinking. (B) Colour photographic images of eye globe during CXL for Epi-off: i) before CXL, ii) UV exposure and iii) UV exposure after the riboflavin absorption; and Epi-on: iv) before CXL, v) UV exposure and vi) UV exposure after the riboflavin absorption.

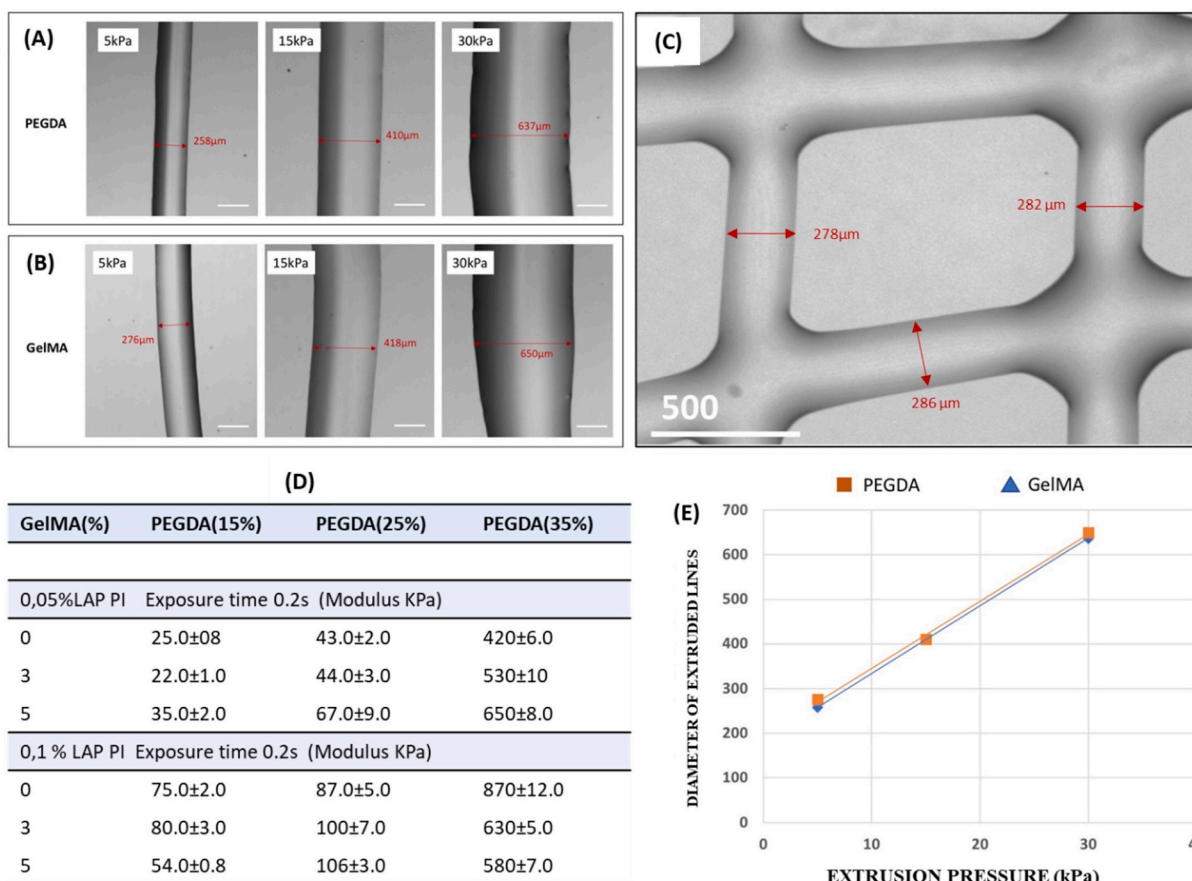


Fig. 5. (A) Optical microscope images of the bioprinted lines with PEGDA and (B) GelMA, for different extrusion pressures. (C) An array of “cross-hatched layers” using the biopen (PEGDA and at 5 kPa). (D) Stiffness values for the proposed bioink formulations: GelMA/PEGDA/PI and (E) Graphic illustrating the diameter of the bioprinted lines in relation to the extrusion pressure.

PI and 0.2s UV exposure (Fig. 5D). For reducing the shear stress, which can reduce the cell viability, we used the tip with a diameter of 400 μm. Bioinks were prepared as described in point 2.4.2. The live/dead assay was employed to visualize the presence of living and dead cells (HCK) and AlamarBlue® was used to determine proliferation rates after 1, 3 and 7 days after printing with the biopen. Positive expression of corneal

stromal keratocyte markers was analyzed by immunofluorescence. Fig. 6A, B and 6C show cell viability and proliferation assays of bioprinted HCK. Cell viability (Fig. 5A) showed homogenous cell distribution with little to no signs of cell death. This was accompanied by cell proliferation over time. Fig. 5D shows the cell viability data for all the bioink combinations tested with (0.1 % PI and 0.2 s UV exposure). It

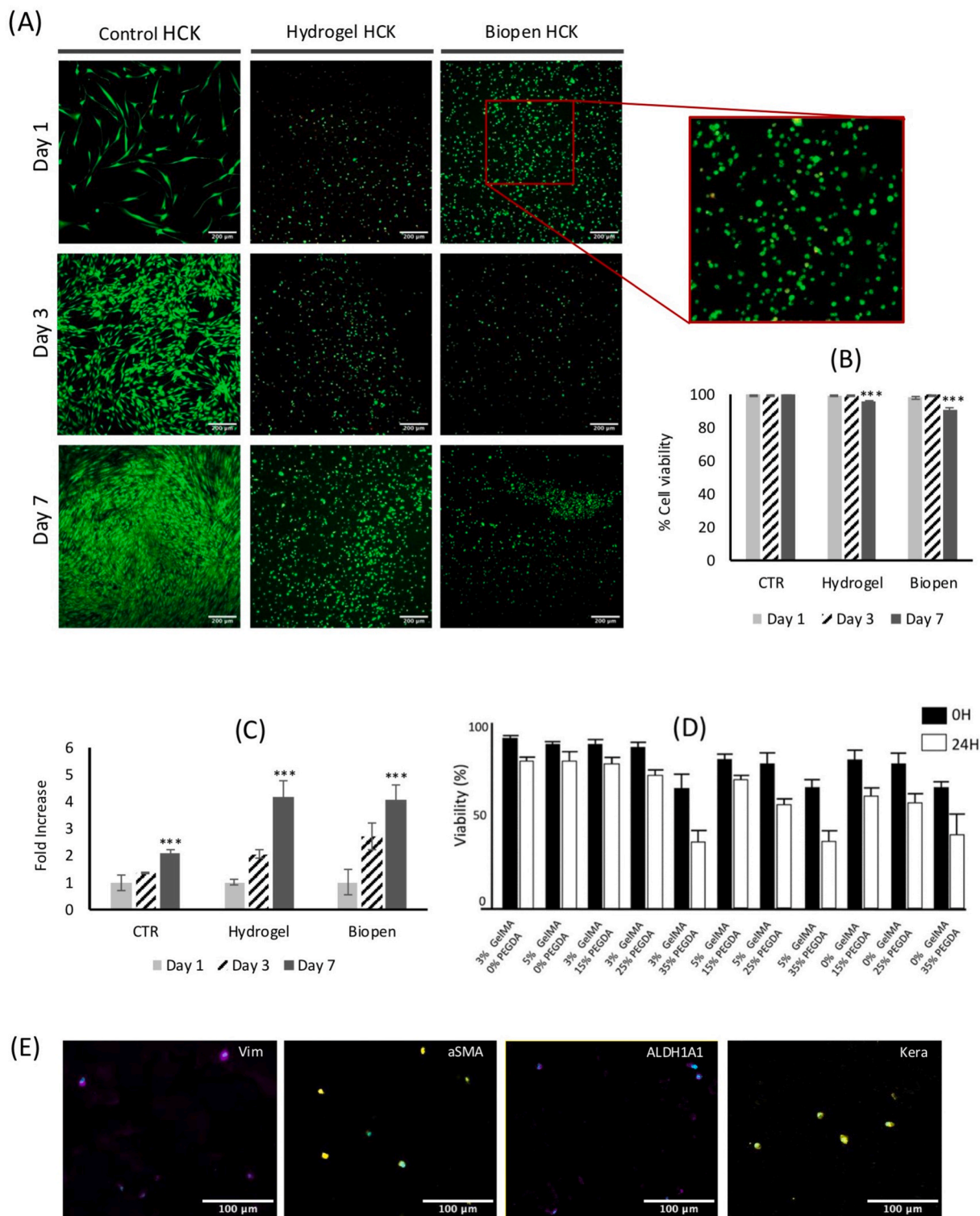


Fig. 6. Viability, proliferation and immunofluorescence assay of HCK. (A) Confocal representative images at day 1, 3 and 7 of Control HCK, Control gel HCK and bioprinted HCK growing in monolayer on GelMA 5%/PEGDA 15%, combination with 0.1 % LAP PI. (B) Graphic show increasing fold change of cell proliferation in all assayed conditions (n = 3; *** indicates p < 0,005). (C) Graphic show quantification of live/dead cells percent at days 1, 3 and 7 after bioprinting. Cell viability data demonstrates that there is no significant difference between the cell viability of the cells embedded in the hydrogel or printed with the biopen, but there is a slight difference from the gel-free control (n = 3; *** indicates p < 0,005). (D) Cell viability data for the all the bioink combinations (0.1 % PI and 0.2 s UV exposure). (Symbols w/v and v/v are factored out in the labels) (E) Representative images of bioprinted HCK at day 7, showing immunofluorescent labeling for HCK markers Vimentin, aSMA, ALDH1A1 and keratocan. Nuclei are counterstained with DAPI (blue).

can be observed that cell viability reduces considerably when increasing the PEGDA percentage on values higher than 25 %. Fig. 5E shows positive expression of the corneal stromal markers ALDH1A1, keratocan, alpha smooth muscle actin (αSMA), and vimentin in the cells encapsulated in the gels, demonstrating no cellular phenotypic dysregulation in the biofabricated culture.

3.3. On cornea direct bioprinting

To demonstrate the potential of our hand-held biopen for corneal wound closure, an injury of dimensions 3 mm × 0.5 mm × 0.2 mm (long x width x depth) was generated into a porcine cornea using 2.75 mm side cut clear corneal knife. We did not use a commercial PEG-based adhesive but start with a solution of 15 % PEGDA and GelMA 5 % which has a similar stiffness (35.0 ± 2.0) than the cornea internal stromal (33 ± 1) and a 0.05 % LAP photoinitiator.

The stiffness of the selected PEGDA/GelMA/PI bionk was modulated to adjust to the cornea stiffness using the UV exposure time parameter in our setup. It was increased and decrease by 0.02s from the previous exposure time (0.2s) used for obtaining the stiffness of 35.0 ± 2.0 kPa (Fig. 7).

The minimum stiffness was at the curing time of 0.18s (34.32 ± 0.78 kPa), and the stiffness increased to 35.13 ± 1.14 kPa (in the case of 0.22 s) as UV exposure time increased. The modulation of stiffness here gives us a strategical advantage for the biomimicry of different microenvironments and mechanical cornea tissue properties. The bioink was bioprinted onto the cornea injury and crosslink using the biopen (Fig. 8). We used the needle of diameter 250 μm and an extrusion rate of 10 μl/s at 5 kPa. These parameters were selected based on the injury dimensions and as per preliminary result showed in Fig. 5.

4. Discussion

The ability of using hand-held biopens to directly control the deposition of biomaterials with or without the presence of live cells during the surgical procedure represents an exciting technical advance in tissue regeneration and replacement. This method stands out for its simplicity and portability, allowing medical professionals to print directly at the injury site with manual control, making them ideal for surgical settings and immediate treatment of complex wounds. This technique could be compared robotic-based *in situ* bioprinting, for example, which offer greater precision and reproducibility due to automation and the use of configurations such as articulated and parallel arms, but require advanced infrastructure and technical expertise to use, while portable

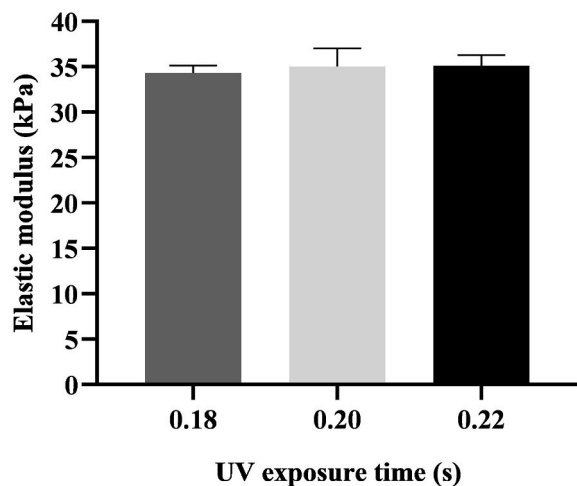


Fig. 7. Elastic modulus of selected PEGDA/GelMA/PI concentration for various UV exposure times (Non-significant differences, $p < 0.05$).

hand-held bioprinters are typically less expensive and therefore more accessible, and simpler to operate [20]. Such bioprinting methodologies are growing supplemented with the development of new biomaterials combinations which aims to replicate the physiology and mechanical properties of human tissues. Some biopens has been developed to meet the bioprinting requirements of surgical printing chondral wound sites, cartilage, and skin applications [26–29]. In particular, the biopen developed in this work shows a great potential for corneal tissue repairing and regeneration and was developed attending the two main corneal tissues: Corneal stroma regeneration and corneal injuries. Corneal stromal regeneration is the main challenge for the total corneal repair. To overcome this issue, in recent times CXL procedure has been developed and results have demonstrated a significantly improvement in the treatment of keratoconus and corneal ectasia. Since new fast corneal crosslink methodologies are emerging, new hand-held tools can be introduced to facilitate the CXL process to surgeons. Iontophoresis corneal collagen cross-linking (I-CXL) is a new non-invasive trans-epithelial technique [23], which seeks to increase the cornea's biomechanical stability by combining an RF ophthalmic solution and UV-A radiation. To boost RF diffusion through the intact epithelium, a local low-intensity electric field is applied. Additionally, to these novel approaches that try to avoid epithelium removal, fast cross-linking using high intensity UV light and shorter periods of time is growing in popularity. Our results envisage the potential of the biopen as a suitable tool for performing the CXL, in particular for fast curing CXL process. The CXL standard protocol (Dresden protocol) was also performed successfully but the long duration of the process due to required illumination time may lack the use of a hand-held tool for such long process. Fast curing in the order of 4–5 min seem to be a reasonable time for a hand-held device. Initial studies suggested that this is an effective and safe process that can represent an alternative to the commonly used Dresden protocol. Although further research and comparison to conventional medical treatment is needed, in particular to determine the effect of variability by movement of the operator, the convention of the biopen and fast crosslinking present high potential in veterinary where the portability could be an advantage over such variability. Corneal ulcers are one of the most common eye problems in the horse and can cause varying degrees of visual impairment. Hellander-Edman, Anna et al. demonstrated the uses of CLX for threatening corneal ulcers in horses. Vision-threatening complications directly associated with the procedure were not observed in their pilot study [24]. Authors believe that further studies on CXL in this species are warranted, with the advantage that it is easy to learn and does not require expertise in microsurgery.

On the other hand, tissue engineering has also allowed the use of different biomaterials for the treatment and regeneration of corneal lesions. Microsurgical suturing of corneal injuries or wounds is often associated with inflammation, which promote vascularization, increasing the risk of infections by microbial agents, among other problems [30,31]. Ocular adhesives ranging from naturally derived polymers (proteins and polysaccharides) to synthetic materials (cyanoacrylates, PEG-based and dendrimers) have been used in ophthalmology from the 80s and are now being demonstrated as an alternative to sutures. These adhesive fluids are usually polymers that are deposited at the ocular injury site and crosslinked (chemically or physically) to hold the tissue. Natural adhesives, including collagen, vitrigel [32,33], fibrin [34], gelatin (GelFilm and GelFoam, GelCore) [35,36], alginate [37], and chitosan [38] have been developed and used for eye regeneration applications. Synthetic PEG-based adhesives have also been extensively used and although they inhibit non-specific binding of cells, the cellular interaction enhancement can be achieved *via* chemical modification by introducing peptide cell binding motifs with PEG-based hydrogels. This flexibility of chemical modification affords a diverse range of functions of PEG-based adhesives. For example, Hoshi et al. have used PEG-based adhesive (FocalSeal® from Genzyme Corporation) for validating an ex-vivo model in porcine eyes. They also validate the process *in vivo* in

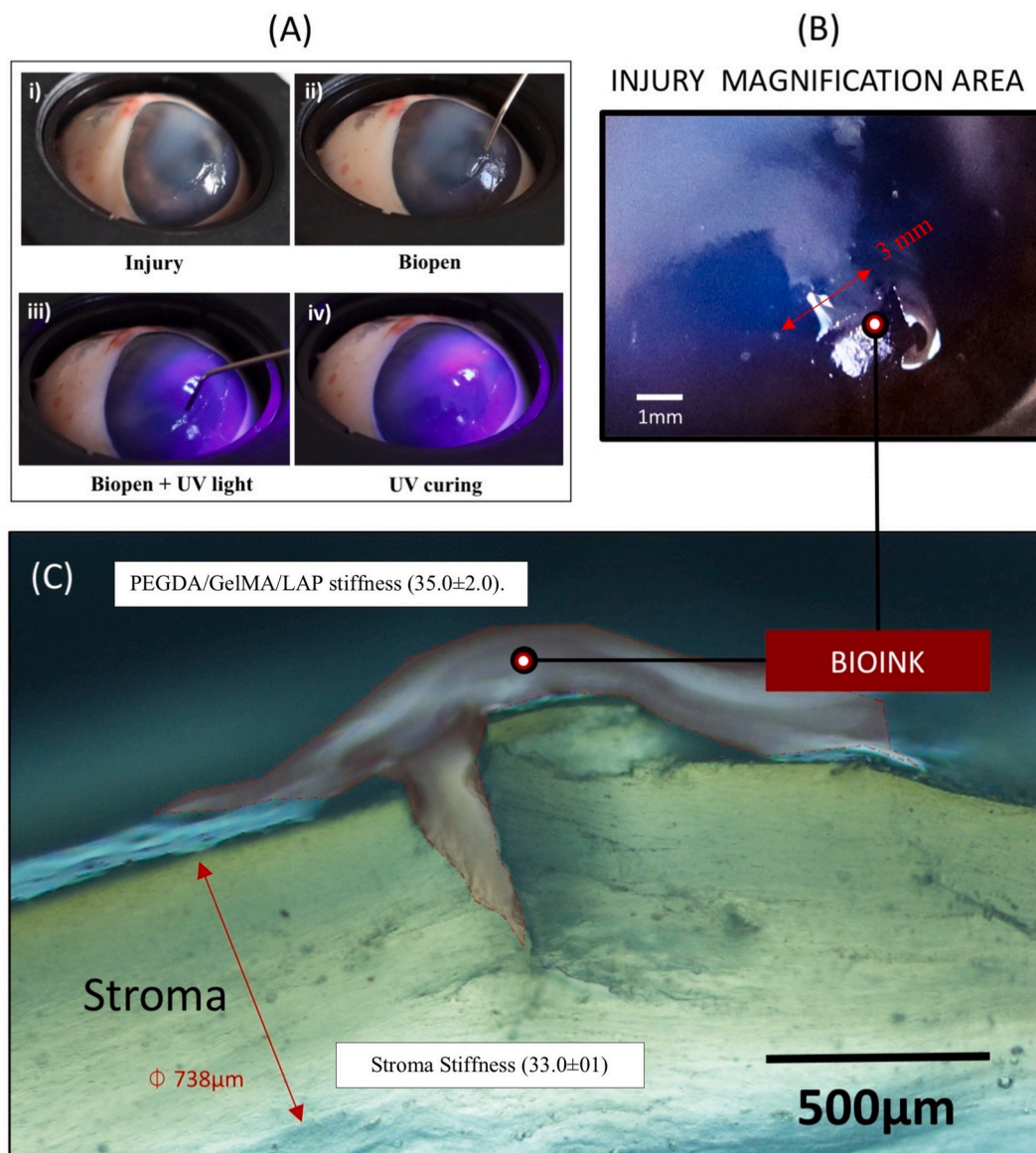


Fig. 8. (A) Application process of PEGDA/GelMA/LAP bioink in a porcine cornea: i) a wound defect in the cornea, ii) the bioink was applied on to the injury using the biopen, iii) the UV light was used to cure while adding the material iv) image of the cornea after printing. B) Magnified image of the cornea after bioprinting and C) Sagittal cornea section image of the injury after bioprinting. PEGDA/GelMA/LAP stiffness (35.0 ± 2.0). Cornea internal stromal stiffness (33 ± 1).

Dutch pigmented rabbit eye models by using a photo-curable PEG-based sealant for the closure of sutureless sclerotomies (surgical incision of the sclera) in microincisional vitrectomy surgery (MIVS). Histological analysis revealed that the PEG-based adhesive did not cause immoderate inflammation [39]. For this reason, this study has also validated the use of the biopen for the application of biomaterials as an alternative to microsurgical suturing, using PEGDA, the base material of the commonly used biomaterials. The results show that the biopen allows the PEGDA to be deposited into the simulated corneal injury, as well as regulating the thickness of the bioink, in a short period, which makes it compatible for clinical use.

Finally, one of the most recently developed strategies involves incorporating primary cell cultures into biomaterials for treating corneal lesions, leveraging their regenerative potential. In fact, several *in vitro* studies have explored the use of HSCs, evaluating their viability and ability to retain a functional phenotype following application in bioprinting techniques [40]. Herein, the developed biopen allows the bioprinting of corneal stromal cells loaded in a light-curing bioink, PEGDA/GelMA/PI, which maintains a high rate of viability and

proliferation after the bioprinting process, as well as the native characteristics markers. These results indicate that the use of biopen as an accurate and guided bioprinting technology could be transferred to the operating room for regenerative purposes in corneal injuries.

The combination of hand-held biopens and the novel photoinitiators opens new avenues for creating customized tissue [41]. Research indicates that various bioinks can be utilized with these devices, enhancing their versatility in creating complex tissue structures (i.e. skin grafts and cartilage). Some newly developed photoinitiators exhibits superior light absorption characteristics and faster polymerization rates compared to conventional initiators [42]. Studies demonstrate that this novel photoinitiators are non-toxic to cells, making it suitable for use in sensitive biological environments. The ability to achieve finer resolution in printed structures is a significant advancement over existing photoinitiators.

While previous studies have highlighted limitations such as slow curing times and cytotoxicity associated with traditional photoinitiators, the novel photoinitiator addresses these issues effectively, leading to improved outcomes in bioprinting. Compared to existing techniques

that often struggle with precision and speed, the integration of the new photoinitiator into hand-held biopens allows for rapid prototyping of complex tissues with high fidelity. Literature on corneal stromal substitutes shows a growing need for materials that mimic natural tissue properties. The ability of novel photoinitiator to create hydrogels with tunable mechanical properties positions it as a promising candidate for developing effective corneal substitutes [43].

5. Conclusions

We have developed a hand-held biopen that can be used for precisely depositing photocrosslinkable biomaterials (RF, PEGDA/GelMA)/PI bioinks into cornea. The biopen was validated for CXL, for cell bioprinting and for corneal wound closure. The typical CXL protocol establishes long time process with stationary lamps to promote crosslinking. In this work, we used the biopen to CXL, as per Dresden Protocol, but also for fast crosslinking processes. Additionally, we demonstrated the possibility of simultaneously controlling the deposition and crosslinking of biomaterials with and without the presence of living cells during surgical treatments. Both biocompatibility and cell viability were demonstrated using HCK, which is a cell type frequently employed in corneal regenerative strategies. The mechanical properties of human cornea can be imitated by tuning the proposed PEGDA/GelMA/PI bioink composition and crosslinking parameters. These results envisage the potential for being translated to a clinical environment for corneal wound closure.

CRedit authorship contribution statement

Nadina Usseglio: Writing – original draft, Investigation. **Lorenzo Moroni:** Writing – review & editing, Methodology. **Daniel Nieto:** Writing – review & editing, Supervision, Methodology, Conceptualization.

Declaration of competing interest

The authors declare that they have no known competing financial interests or personal relationships that could have appeared to influence the work reported in this paper.

Acknowledgement

Daniel Nieto thanks to European Research Council Consolidator Grant (101125172 HOT-BIOPRINTING- HE-ERC-2023COG). Daniel Nieto is supported by the Oportunus Programme (Xunta de Galicia) since 2024. Lorenzo Moroni is grateful to the Dutch Province of Limburg and to the European Research Council starting grant “Cell Hybridge” (Grant #637308).

Data availability

No data was used for the research described in the article.

References

- [1] L. Moroni, et al., Biofabrication: a guide to technology and terminology, *Trends Biotechnol.* 36 (2018) 384–402.
- [2] J. Groll, et al., Biofabrication: reappraising the definition of an evolving field, *Biofabrication* 8 (2016).
- [3] Sorosh Derakhshanfara, Rene Mbelecka, Kaige Xua, Xingying Zhanga, Wen Zhongb Malcolm Xinga 3D bioprinting for biomedical devices and tissue engineering: a review of recent trends and advances, *Bioact. Mater.* 3 (2) (2018) 144–156.
- [4] G. Brunello, et al., Powder-based 3D printing for bone tissue engineering, *Biotechnol. Adv.* 34 (2016) 740–753.
- [5] S. Bose, et al., Bone tissue engineering using 3D printing, *Mater. Today* 16 (2013) 496–504.
- [6] Z. Zhou, et al., Printability of calcium phosphate: calcium sulfate powders for the application of tissue engineered bone scaffolds using the 3D printing technique, *Mater. Sci. Eng. C* 38 (2014) 1–10.
- [7] J.A. Inzana, et al., 3D printed bioceramics for dual antibiotic delivery to treat implant-associated bone infection, *Eur. Cell. Mater.* 30 (2015) 232–247.
- [8] T. Xu, et al., Hybrid printing of mechanically and biologically improved constructs for cartilage tissue engineering applications, *Biofabrication* 5 (2012) 01500.
- [9] S. Michael, et al., Tissue engineered skin substitutes created by laser-assisted bioprinting form skin-like structures in the dorsal skin fold chamber in mice, *PLoS One* 8 (2013) e57741.
- [10] J. Soumen, A. Lerman, Bioprinting a cardiac valve, *Biotechnol. Adv.* 33 (2015) 1503–1521.
- [11] Z. Zhang, et al., 3D bioprinting of soft materials-based regenerative vascular structures and tissues, *Composites, Part B* 123 (2017) 279–291.
- [12] E.L. Nyberg, et al., 3D-printing technologies for craniofacial rehabilitation, reconstruction, and regeneration, *Ann. Biomed. Eng.* 45 (2017) 45–57.
- [13] E. Provaggi, et al., Applications of 3D printing in the management of severe spinal conditions, *Proc. Inst. Mech. Eng. Part H J. Eng. Med.* 231 (2017) 471–486.
- [14] A. Popov, et al., 3D bioprinting for musculoskeletal applications. *J. 3D Print. Méd.* 1 (2017) 191–211.
- [15] L. Hayman, et al., Tissue engineering in hand surgery: a technology update, *J. Hand Surg. Am.* 42 (2017) 727–735.
- [16] Z.M. Jessop, et al., 3D bioprinting for reconstructive surgery: principles, application, and challenges, *J. Plast. Reconstr. Aesthetic Surg.* 70 (2017) 1155–1170.
- [17] N. Zhong, X. Zhao, 3D printing for clinical application in otorhinolaryngology, *Eur. Arch. Oto-Rhino-Laryngol.* 274 (2017) 4079–4089.
- [18] K. Gulati, S. Ivanovski, Dental implants modified with drug releasing titania nanotubes: therapeutic potential and developmental challenges, *Expert Opin. Drug Deliv.* 14 (2017) 1009–1024.
- [19] K. Miri Amir, Daniel Nieto, Luis Iglesias, et al., Microfluidics-Enabled multi-material maskless stereolithographic bioprinting, *Adv. Mater.* (2018) 1800242.
- [20] Z. Pazhouhnia, N. Beheshtizadeh, M.S. Namini, N. Lotfikhshahesh, Portable hand-held bioprinters promote in situ tissue regeneration, *Bioeng Transl Med* 7 (3) (2022) e10307.
- [21] C.D. O’Connell, C. Di Bella, F. Thompson, C. Augustine, S. Beirne, R. Cornock, C. J. Richards, J. Chung, S. Gambhir, Z. Yue, J. Bourke, B. Zhang, A. Taylor, A. Quigley, R. Kapsa, P. Choong, G.G. Wallace, Development of the Biopen: a handheld device for surgical printing of adipose stem cells at a chondral wound site, *Biofabrication* 8 (1) (2016 Mar 23) 015019.
- [22] Rúben F. Pereira, Paulo J. Bá, et al., 3D photo-fabrication for tissue engineering and drug delivery, *Engineering* 1 (1) (2015) 90–112.
- [23] A. Cantemir, A.I. Alexa, N. Anton, et al., Evaluation of iontophoretic collagen cross-linking for early stage of progressive keratoconus compared to standard cross-linking: a non-inferiority study, *Ophthalmol Ther* 6 (1) (2017) 147–160, <https://doi.org/10.1007/s40123-017-0076-8>.
- [24] A. Hellander-Edman, K. Makdoui, J. Mortensen, B. Ekesten, Corneal cross-linking in horses with ulcerative keratitis, *BMC Vet. Res.* 9 (2013) 128.
- [25] M. Islam, O. Buznyk, J.C. Reddy, N. Pasychnikova, E.I. Alarcon, S. Hayes, P. Lewis, P. Fagerholm, C. He, S. Iakymenko, W. Liu, K.M. Meek, V.S. Sangwan, M. Griffith, Biomaterials-enabled cornea regeneration in patients at high risk for rejection of donor tissue transplantation, *NPJ Regen. Med.* 3 (2018) 2.
- [26] P. Gain, R. Jullienne, Z. He, M. Aldossary, S. Acquart, F. Cognasse, G. Thuret, Global survey of corneal transplantation and eye banking, *JAMA Ophthalmol.* 134 (2016) 167–173.
- [27] C.D. O’Connell, C. Di Bella, F. Thompson, C. Augustine, S. Beirne, R. Cornock, et al., Development of the biopen: a handheld device for surgical printing of adipose stem cells at a chondral wound site, *Biofabrication* 8 (2016) 015019, 2016.
- [28] S. Duchi, C. Onofrillo, C.D. O’Connell, R. Blanchard, C. Augustine, A.F. Quigley, et al., Handheld co-axial bioprinting: application to in situ surgical cartilage repair, *Sci. Rep.* 7 (2017) 5837, 2017.
- [29] N. Hakimi, R. Cheng, L. Leng, M. Sotoudehfar, P.Q. Ba, N. Bakhtyar, et al., Handheld skin printer: in situ formation of planar biomaterials and tissues, *Lab Chip* 18 (2018) 1440–1451.
- [30] A.V. Ljubimov, M. Saghizadeh, Progress in corneal wound healing, *Prog. Retin. Eye Res.* 49 (2015) 17–45.
- [31] E. Spoerl, M. Huhle, Seiler T Induction of cross-links in corneal tissue, *Exp. Eye Res.* 66 (1998) 97–103.
- [32] T. Seiler, F. Hafezi, Corneal cross-linking-induced stromal demarcation line, *Cornea* 25 (2006) 1057–1059.
- [33] G. Wollensak, E. Spoerl, T. Seiler, Riboflavin/ultraviolet-a-induced collagen crosslinking for the treatment of keratoconus, *Am. J. Ophthalmol.* 135 (2003) 620–627.
- [34] F. Cifariello, M. Minicucci, F. Di Renzo, et al., Epi-off versus epi-on corneal collagen cross-linking in keratoconus patients: a comparative study through 2-year follow-up, *J Ophthalmol* 2018 (2018) 4947983.
- [35] A. Moramarco, A. Iovieno, A. Sartori, L. Fontana, Corneal stromal demarcation line after accelerated crosslinking using continuous and pulsed light, *J. Cataract Refract. Surg.* 41 (2015) 2546–2551.
- [36] D. Zadok, Y. Goldich, Y. Barkana, A. Rasko, I. Avni, Influence of UV-A-riboflavin corneal collagen crosslinking on biomechanical properties of keratoconic eyes, in: Paper Presented at the 2008 ASCRS Annual Meeting, 2008. Chicago.
- [37] L.J. Müller, E. Pels, G.F. Vrensen, The specific architecture of the anterior stroma accounts for maintenance of corneal curvature, *Br. J. Ophthalmol.* 85 (2001) 437–443.

- [38] D.A. Luce, Determining in vivo biomechanical properties of the cornea with an ocular response analyzer, *J. Cataract Refract. Surg.* 31 (2005) 156–162.
- [39] E. Albe, Measuring corneal biomechanical properties in keratoconic eyes undergoing crosslinking, *Cataract and Refractive Surgery Today Europe* 5 (2008) 33–34.
- [40] H. Gómez-Fernández, F. Alhakim-Khalak, S. Ruiz-Alonso, et al., Comprehensive review of the state-of-the-art in corneal 3D bioprinting, including regulatory aspects, *Int. J. Pharm.* 662 (2024) 124510.
- [41] W. Fang, Z. Yu, G. Gao, M. Yang, X. Du, Y. Wang, Q. Fu, Light-based 3D bioprinting technology applied to repair and regeneration of different tissues: a rational proposal for biomedical applications, *Mater Today Bio* 27 (2024 Jun 26) 101135.
- [42] K. Ikhoury, J. Zuazola, S. Vijayavenkataraman, Bioprinting the future using light: a review on photocrosslinking reactions, photoreactive groups, and photoinitiators, *SLAS Technol* 28 (3) (2023 Jun) 142–151.
- [43] Tamás Monostori, Diána Szűcs, Borbála Lovászi, Lajos Kemény, Zoltán Veréb, Advances in tissue engineering and 3D bioprinting for corneal regeneration, *International Journal of Bioprinting* 10 (2) (2024) 1669.